Conformational Changes of an Exchangeable Apolipoprotein, Apolipophorin III from *Locusta migratoria*, at Low pH: Correlation with Lipid Binding†

Paul M. M. Weers,‡ Cyril M. Kay,§ and Robert O. Ryan*,‡

Lipid Biology in Health and Disease Research Group, Children's Hospital Oakland Research Institute, 5700 Martin Luther King Jr. Way, Oakland, California 94609, and Protein Engineering Network of Centres of Excellence, Department of Biochemistry, University of Alberta, Edmonton, Alberta, Canada

Received February 27, 2001; Revised Manuscript Received April 27, 2001

ABSTRACT: *Locusta migratoria* apolipophorin III (apoLp-III) is a helix bundle exchangeable apolipoprotein that reversibly binds to lipoprotein surfaces. Structural reorganization of its five amphipathic α-helices enables the transition from the lipid-free to lipid-bound state. ApoLp-III-induced transformation of dimyristoylphosphatidylcholine (DMPC) bilayer vesicles into smaller discoidal complexes is enhanced as a function of decreasing pH, with maximal transformation occurring at pH 3.5. Over the entire pH range studied, apoLp-III retains nearly all of its secondary structure content. Whereas no changes in fluorescence emission maximum of the two Trp residues in apoLp-III were observed in the pH range from 7.0 to 4.0, a further decrease in pH resulted in a strong red shift. Near-UV circular dichroism spectra of apoLp-III showed well-defined extrema (at 286 and 292 nm) between pH 7.0 and pH 4.0, which were attributed to Trp115. Below pH 4.0, these extrema collapsed, indicating a less rigid environment for Trp115. Similarly, the fluorescence intensity of 8-anilinonaphthalene-1-sulfonate in the presence of apoLp-III increased 4-fold below pH 4.0, indicating exposure of hydrophobic sites in the protein in this pH range. Taken together, the data suggest two conformational states of the protein. In the first state between pH 7.0 and pH 4.0, apoLp-III retains a nativelike helix bundle structure. The second state, found between pH 3.0 and pH 4.0, is reminiscent of a molten globule, wherein tertiary structure contacts are disrupted without a significant loss of secondary structure content. In both states DMPC vesicle transformation is enhanced by lowering the solution pH, reaching an optimum in the second state. The correlation between tertiary structure and lipid binding activity suggests that helix bundle organization is a determinant of apoLp-III lipid binding activity.

Apolipophorin III (apoLp-III)[1] from the locust *Locusta migratoria* is a model exchangeable apolipoprotein that exists in alternate lipid-free and lipid-associated states. Structural studies of apoLp-III in the absence of lipid reveal a globular bundle of five amphipathic α-helices (*1*). Hydrophobic amino acid side chains are buried in the bundle interior and, thus, are sequestered from the aqueous environment. On the other hand, polar and charged amino acid side chains are exposed to buffer, consistent with the water solubility of the globular helix bundle. It is postulated that lipid binding induces a significant reorganization of helical segments, allowing interaction of the hydrophobic face of amphipathic α-helices with the lipid surface (*2*, *3*). The antiparallel, up-and-down, helix topology of *L. migratoria* apoLp-III is consistent with the hypothesis that, upon interaction with a lipid surface, the helix bundle opens in a reversible manner, about loop segments that connect helices in the bundle (*1*, *4*).

ApoLp-III interaction with phospholipid vesicles provides a useful system to study the molecular basis of its lipid binding property. When added to unilamellar vesicles of dimyristoylphosphatidylcholine (DMPC) at the gel to liquid-crystalline phase transition temperature of DMPC, apoLp-III induces transformation of the vesicles into discoidal complexes (*5*). Characterization of the discoidal complexes by electron microscopy, circular dichroism (CD), and fluorescence and Fourier transformed infrared spectroscopy has led to a model of the lipid-bound conformation of apoLp-III in which the protein adopts an open conformation, circumscribing the periphery of the disk in a belt-like manner (*4*, *6*, *7*). At present, however, it is not known what factors modulate the ability of apoLp-III to form a stable binding interaction with lipid surfaces. Studies with other lipid binding proteins have shown that interaction with lipid surfaces is increased under acidic pH conditions (*8*, *9*). In the present studies, we demonstrate that the rate of *L. migratoria* apoLp-III-induced vesicle transformation is significantly enhanced as a function of decreasing pH. Further, taking advantage of the unique spectroscopic properties of

† Supported by a grant from the National Institutes of Health (HL64159).

* To whom correspondence should be addressed. Tel: 510-450-7645. Fax: 510-450-7910. E-mail: rryan@chori.org.

‡ Children's Hospital Oakland Research Institute.

§ University of Alberta.

[1] Abbreviations: ANS, 8-anilinonaphthalene-1-sulfonate; apoLp-III, apolipophorin III; CD, circular dichroism; EM, electron microscopy; DMPC, dimyristoylphosphatidylcholine; λ_{max}, fluorescence emission maximum.

10.1021/bi010410f CCC: $20.00
Published on Web 05/31/2001

this protein, we characterize the correlation between apoLp-III tertiary structure alterations and increased lipid binding activity.

MATERIALS AND METHODS

Proteins. Recombinant *L. migratoria* apoLp-III was expressed in *Escherichia coli* as described previously (*10*) and purified by reversed-phase HPLC on a linear gradient of water−acetonitrile, using a Zorbax C8 column. Purity of the isolated protein was verified by analytical HPLC and sodium dodecyl sulfate−polyacrylamide gel electrophoresis. Protein concentration was measured using the bicinchoninic acid protein assay (Pierce Chemical Co., Rockford, IL).

Spectroscopy. Fluorescence spectroscopy was carried out in a Shimadzu RF-5301 spectrofluorophotometer or a Perkin-Elmer LS-50B luminescence spectrometer. ApoLp-III tryptophan residues were excited at 280 nm (3 nm slit width) with emission monitored between 290 and 500 nm (3 nm slit width). Sample temperature was maintained at 25 °C in a temperature controlled cuvette holder. Tryptophan fluorescence emission maximum (λ_{max}) values were the average ± 1 nm of three determinations. Experiments with 8-anilinonaphthalene-1-sulfonate (ANS) were carried out in 100 mM citrate of a given pH with 250 μM ANS and 5.6 μM apoLp-III. Excitation was set at 395 nm and emission monitored between 400 and 600 nm (6 nm slit width).

Near- and far-UV circular dichroism (CD) spectra were obtained on a Jasco J-720 spectropolarimeter calibrated with 0.06% ammonium *d*-camphor-10-sulfonate as described (*6*). The temperature of the sample was maintained at 25 °C using a Lauda RM6 low-temperature circulator. Protein samples were dissolved in 100 mM citrate, pH 2.3−6. For pH values between 5 and 7.5, proteins were dissolved in 100 mM sodium phosphate. No differences in spectral properties were observed when proteins were analyzed in citrate or sodium phosphate.

Phospholipid Vesicle Transformation. Substrate DMPC vesicles were prepared by extrusion as described elsewhere (*5*). ApoLp-III was dissolved in 20 mM Tris-HCl, pH 7.2, 150 mM NaCl, and 0.5 mM EDTA. Phospholipid (500 μg) and protein (200 μg) were mixed in a thermostated cuvette containing 20 mM Tris-HCl and 150 mM NaCl, pH 7.2, or 100 mM citrate buffers of the appropriate pH. In experiments where GdnHCl was used, the solution was buffered in 100 mM sodium phosphate, pH 7.5. Changes in sample turbidity were monitored by right angle light scattering on a Shimadzu spectrofluorophotometer (RF-5301) with the excitation and emission monochromator set at 580 nm. First-order rate constants (k) were obtained from the slope of a plot of the logarithm of light scatter intensity versus time, while the time needed for 50% clearance ($t_{1/2}$) equals $1/k$.

Electron Microscopy. ApoLp-III (1 mg) and DMPC vesicles (2.5 mg) were incubated for 16 h at 24 °C and isolated by KBr density gradient ultracentrifugation. Following dialysis against 50 mM sodium phosphate, pH 7.5, complexes were adsorbed to hydrophilized carbon-coated grids and rinsed three times in 10 mM Tris-HCl, 10 mM NaCl, and 1.5 mM $MgCl_2$, pH 7.0. The grids were negatively stained for 10 s with 2% sodium phosphotungstate, pH 7.0, and photographed in a Philips EM 420 operated at 100 kV.

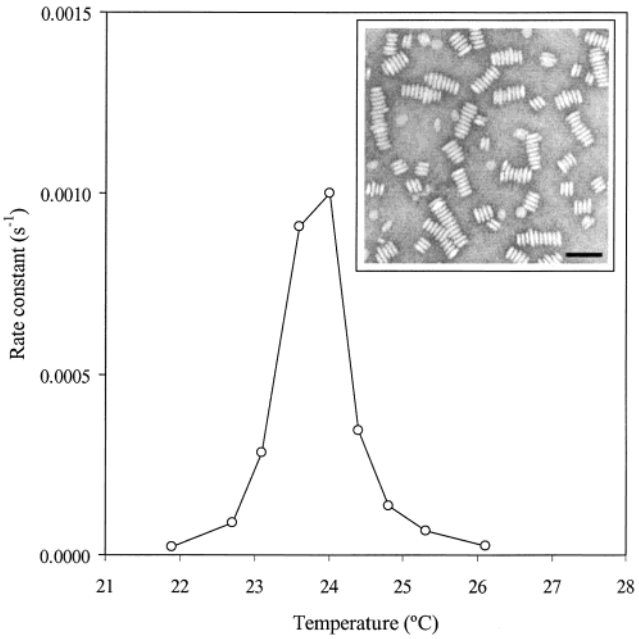

FIGURE 1: Effect of temperature on DMPC clearance rates by apoLp-III (80:1 molar ratio). Rate constants (k) were calculated assuming first-order kinetics. Inset: EM micrograph of DMPC−apoLp-III complexes (bar equals 50 nm).

RESULTS

ApoLp-III Interaction with DMPC Vesicles. One of the hallmark characteristics of exchangeable apolipoproteins is an ability to transform phospholipid bilayer vesicles into discoidal complexes. Although *L. migratoria* apoLp-III functions in diacylglycerol transport in vivo (*11*), it also interacts strongly with phospholipid vesicles. Addition of apoLp-III to a turbid suspension of unilamellar DMPC vesicles at 24 °C induces a rapid decrease in light scatter intensity due to formation of much smaller lipid−protein complexes. As shown in Figure 1, apoLp-III-induced DMPC vesicle transformation rate is dependent on temperature. Maximal clearance rates were observed at approximately 24 °C, near the DMPC gel−liquid-crystalline phase transition temperature (23.9 °C). Although reaction rates remained high within 1 °C of the phospholipid transition temperature, beyond this range 10-fold lower reaction rates were observed. Negative stain electron microscopy of the transformation product (Figure 1, inset) revealed the presence of discrete discoidal particles with a diameter of 19.3 ± 2.4 nm.

Effect of Solution pH on ApoLp-III-Induced DMPC Vesicle Transformation. To further characterize apoLp-III-induced DMPC vesicle transformation activity, we examined the effect of solution pH on vesicle transformation rate (Figure 2A). Whereas charged moieties in the DMPC phosphocholine headgroup have pK_a values <2.5, apoLp-III may be susceptible to subtle pH-induced conformational alterations that affect its lipid binding properties. Starting from pH 7.2, the rate of apoLp-III-induced DMPC vesicle transformation increased steadily as the solution pH decreased, with a maximum rate observed at pH 3.5 (Figure 2B). A further decrease in solvent pH to 2.3 resulted in a significant reduction in transformation rate. Electron micrographs demonstrated that the apoLp-III-dependent decrease in sample light scattering at pH 3.5 resulted from formation of discoidal complexes (data not shown).

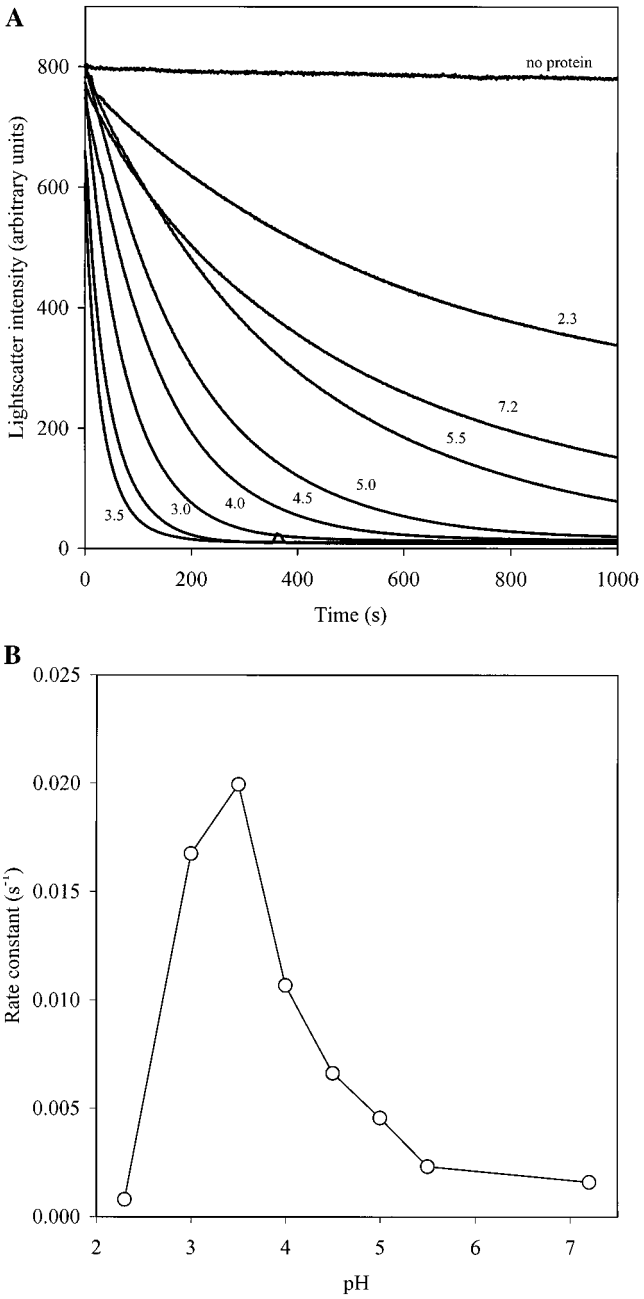

FIGURE 2: Effect of pH on DMPC clearance rates. Panel A: apoLp-III was incubated in the presence of DMPC vesicles at various solution pHs, inducing the formation of much smaller discoidal complexes. The decrease in sample turbidity induced by apolipoprotein was measured by light scattering. Panel B: Rate constants of DMPC vesicle transformation as a function of pH.

Effect of pH on ApoLp-III Trp Fluorescence. The enhanced ability of apoLp-III to induce DMPC vesicle transformation as a function of decreasing pH may be related to changes in protein secondary or tertiary structure. In the pH range studied, apoLp-III maintains its secondary structure content (*6*). ApoLp-III Trp fluorescence λ_{max} was used to probe for pH-induced apolipoprotein tertiary structural alterations. *L. migratoria* apoLp-III (164 residues) contains two tryptophan residues located at positions 115 and 130, while no Tyr is present. Two single tryptophan mutants, apoLp-III-W at position 115 and apoLp-III-W at position 130 (*12*), were used to monitor changes in protein tertiary structure. The wavelength of maximum fluorescence emission of apoLp-III-W

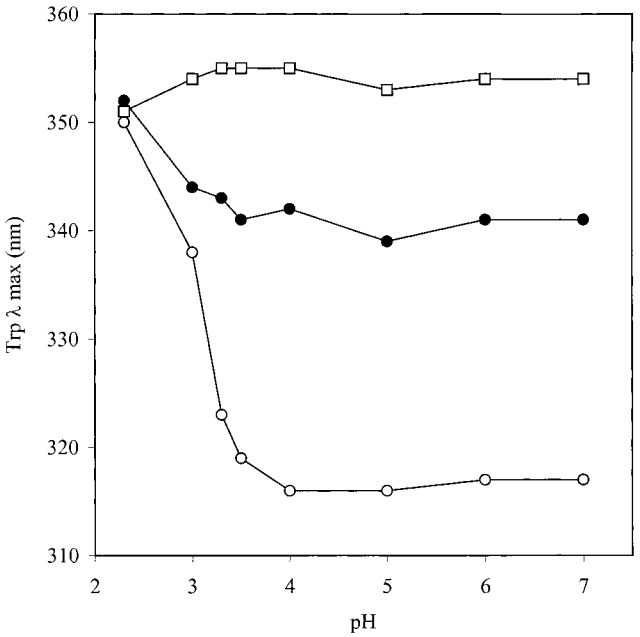

FIGURE 3: Trp fluorescence λ_{max} to monitor changes in apolipoprotein structure induced by a decrease in pH. Trp was excited at 280 nm, and emission maxima (λ_{max}) were followed as a function of pH. Shown are two single Trp apoLp-III mutants, apoLp-III-W at position 115 (open circles) and apoLp-III-W at position 130 (closed circles), and free L-Trp (open squares).

at position 115 is 317 nm at neutral pH (excitation 280 nm), a result of its buried location in the globular helix bundle fold and its positioning in the center of the long axis of helix H4 (*12*). Between pH 7.2 and pH 4.0, the λ_{max} of Trp115 in apoLp-III remained unchanged (Figure 3). By contrast, at pH values below 4.0, a strong red shift in the wavelength of maximum fluorescence emission was observed, indicating exposure of Trp115 to the aqueous environment. At pH 2.3 Trp115 λ_{max} was red shifted by 30 nm, reaching a value similar to that of L-Trp (354 nm), suggesting complete solvent exposure of Trp115. Whereas Trp115 is buried in the helix bundle fold of apoLp-III, Trp130 is located in the loop connecting helices H4 and H5 (*1*). As a result of its partial exposure to the aqueous environment, the λ_{max} of Trp 130 is higher at neutral pH (340 nm). As with Trp115, no shift in the wavelength of maximum fluorescence was observed for apoLp-III-W at position 130 between pH 7.2 and pH 4.0. At pH <4 the λ_{max} of Trp130 increases, reaching 350 nm at pH 2.3 (10 nm red shift).

Aromatic CD Spectral Changes as a Function of pH. L. migratoria apoLp-III gives rise to exceptionally well-defined aromatic CD spectra, displaying extrema at 286 and 292 nm (Figure 4). This is the result of the buried location of Trp115, causing restriction in side-chain mobility of the indole ring, combined with the absence of Cys and Tyr in this protein (*12*). The unique near-UV spectral properties of Trp115 were exploited to further study apolipoprotein structure as a function of solution pH. It is expected that side-chain mobility of Trp115 will become less restrained if the protein adopts a more flexible conformation. Increased flexibility of Trp115 would be reflected by near-UV CD spectral changes (*12*). Figure 4 (inset) shows aromatic CD spectra of apoLp-III at different pH values. The intensity of the extrema at 286 and 292 nm remained well defined until the solvent pH was decreased to 3.6. Below pH 3.6, the intensity

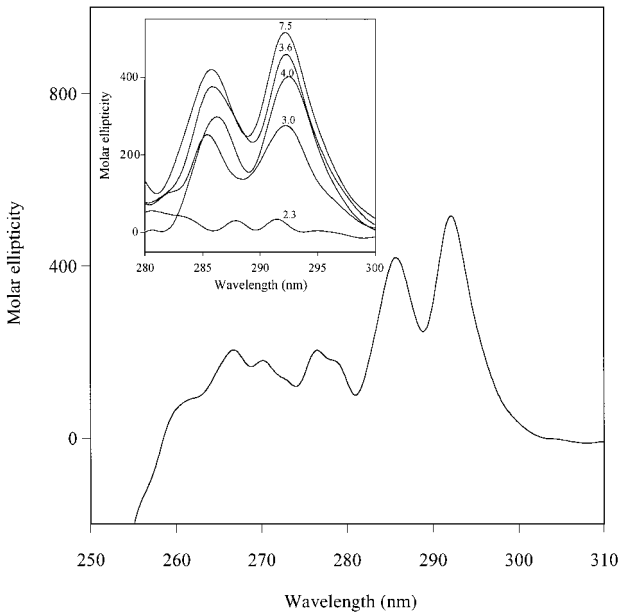

FIGURE 4: Aromatic CD spectrum of apoLp-III. *L. migratoria* apoLp-III displays strong extrema at 286 and 296 nm that can be attributed to Trp-115. Inset: apoLp-III at various pH conditions showing the molar ellipticity between 280 and 300 nm at pH 7.5, 4.0, 3.6, 3.0, and 2.3.

of the extrema at 286 and 292 nm decreased significantly, indicating that Trp115 side-chain mobility has become less restricted. At pH 2.3, near-UV spectral properties of apoLp-III-W at position 115 become similar to that of apoLp-III-W at position 130 (*12*), lacking the well-defined extrema at 286 and 292 nm.

Effect of pH on ApoLp-III-Induced ANS Fluorescence Enhancement. The extrinsic hydrophobic fluorescent probe, ANS, binds to clustered hydrophobic residues and has been widely used to detect molten globule states in proteins (*13*). Hydrophobic residues in the helix bundle state of apoLp-III form a continuum directed toward the interior of the bundle. It is conceivable that a pH-induced change in amphipathic α-helix packing in the bundle results in increased exposure of the hydrophobic interior of apoLp-III, as suggested by changes in the fluorescence properties of apoLp-III Trp residues at pH <4. In buffer alone, ANS displays weak fluorescence intensity over the pH range from 2 to 7, with a λ_{max} of ~520 nm (curve c, Figure 5A). Addition of apoLp-III at pH 6.2 results in a large blue shift (λ_{max} 467 nm) and an increase in fluorescence intensity (curve a). When the pH was lowered to 2.3, an equivalent amount of apoLp-III induced an additional 4-fold increase in ANS fluorescence intensity (curve b). Further characterization of this effect (Figure 5B) revealed that, between pH 7.2 and pH 4.0, ANS fluorescence intensity increased slightly upon addition of apoLp-III. On the other hand, below pH 4 the acidic conditions induced dramatic increases in ANS fluorescence intensity of apoLp-III samples. At pH 1.9, ANS fluorescence intensity was slightly reduced, which may indicate loss of apoLp-III secondary structure and subsequent loss of clustered hydrophobic surface.

Stability of ApoLp-III. Acidic conditions might induce a decrease in apoLp-III stability, reducing the energy barrier for insertion into the phospholipid bilayer and increasing vesicle transformation rates. Previous far-UV CD studies,

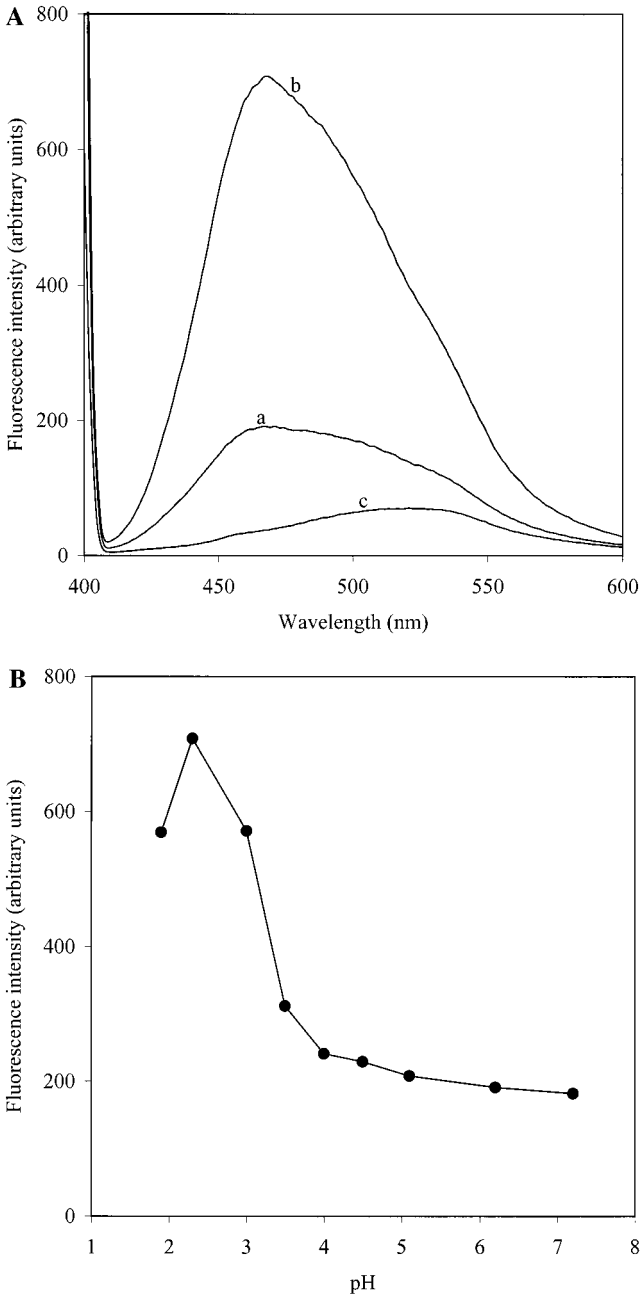

FIGURE 5: ANS binding to apoLp-III. Protein samples were excited at 395 nm, and emission was monitored using a slit width of 6 nm. Panel A: ANS fluorescence emission profile of apoLp-III in the presence of ANS at pH 6.2 (curve a) and pH 2.3 (curve b). ANS fluorescence in the absence of apolipoprotein is also shown (curve c). Panel B: ApoLp-III-dependent ANS fluorescence intensity at 467 nm as a function of pH.

however, showed that negative ellipticity at 221 nm remains largely unaffected over a pH range from 3 to 7 (*6*). In accordance with this, GdnHCl-induced denaturation curves of apoLp-III secondary structure determined at pH values between pH 7 and pH 3 showed little variation, each displaying a denaturation midpoint of ~0.6 M GdnHCl (Figure 6). However, inclusion of 0.3 M GdnHCl to a solution of apoLp-III resulted in a significant increase in DMPC vesicle transformation rate (Figure 6, inset). This GdnHCl molarity has only small effects on apoLp-III secondary structure content (*6*) and induces a small red shift in Trp fluorescence λ_{max} of apoLp-III-W at position 115 and

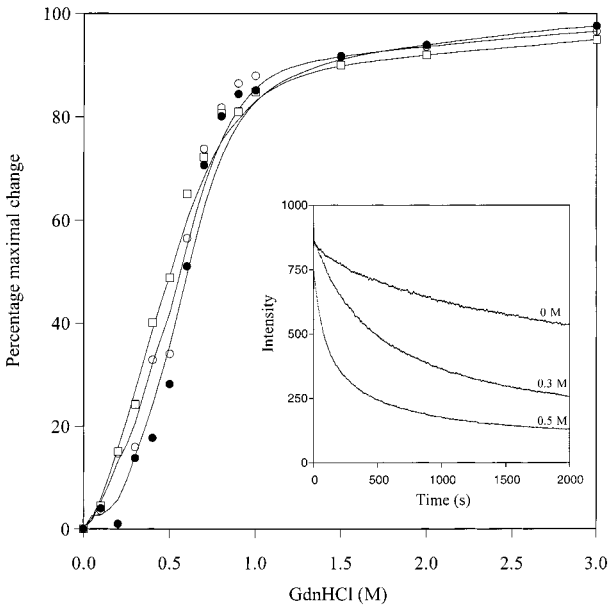

FIGURE 6: GdnHCl-induced denaturation of apoLp-III at various solution pHs. ApoLp-III samples were incubated overnight with different concentrations of GdnHCl at pH 7.0 (open circles), pH 5.0 (closed circles), and pH 3.0 (open squares). The extent of apolipoprotein denaturation was monitored by far-UV CD. Inset: Effect of GdnHCl on DMPC transformation rates. ApoLp-III was dissolved in 100 mM sodium phosphate buffer at pH 7.5 in the presence of GdnHCl and added to DMPC vesicles at the GdnHCl concentration indicated.

Table 1: Trp Fluorescence λ_{max} of ApoLp-III at Position 115 as a Function of GdnHCl[a]

GdnHCl (M)	red shift (nm)	% change of maximum	GdnHCl (M)	red shift (nm)	% change of maximum
0	0		0.6	23.3	76.1
0.1	0		0.7	27.2	88.9
0.2	1.3	1.6	0.8	28.0	91.5
0.3	3.9	4.3	0.9	29.0	94.8
0.4	6.9	22.6	1.0	30.6	100
0.5	15.3	50.0			

[a] λ_{max} = 317 nm at 0 M GdnHCl in 100 mM sodium phosphate at pH 7.2.

apoLp-III-W at position 130 (Table 1). At 0.5 M GdnHCl, close to the midpoint of GdnHCl-induced denaturation, clearance rates are increased 10-fold compared to incubations in the absence of GdnHCl. Thus, changes in structure induced by GdnHCl create a loosely folded conformation that displays enhanced ability to interact with DMPC vesicles.

DISCUSSION

ApoLp-III plays a key role in insect lipoprotein metabolism where it cycles between lipid-free and lipoprotein-associated states (*11*). On the basis of several unique features of this protein, it has been employed as a model apolipoprotein for structure−function studies (*3*). First, the availability of a high-resolution X-ray crystal structure for the full-length protein is a major advantage, allowing targeting of specific microdomains in the protein. Second, high yields of recombinant apoLp-III are readily obtained in *E. coli*. Indeed, after induction of protein expression and cleavage of the vector-encoded pelB leader peptide, apoLp-III escapes the bacteria and specifically accumulates in the culture medium at concentrations up to 200 mg of protein/L (*10*). Third, the lack of apoLp-III self-association, even under high protein concentrations (>10 mg/mL), facilitates biophysical studies (*6*). In addition, structural similarity exists between the N-terminal domain of human apoE and apoLp-III. ApoE is a more complex apolipoprotein, involved in lipoprotein metabolism and neurobiology (*14*, *15*). Full-length apoE is comprised of two structural domains, an N-terminal receptor binding domain and a C-terminal domain with high lipid binding affinity. The structure of the N-terminal domain has been resolved (*16*) and, like apoLp-III, exists as a globular helix bundle in the absence of lipid.

Incubation of apoLp-III with DMPC bilayer vesicles induces formation of stable disk-shaped lipid−protein complexes. The formation of these complexes, which is conveniently monitored by changes in sample light scattering, is dependent on temperature and pH. As shown previously for human apoA-I (*17*), optimal vesicle transformation rates are observed when the reaction is carried out at or near the gel−liquid-crystalline phase transition temperature of DMPC. The diameter of *L. migratoria* apoLp-III−DMPC disks was estimated by electron microscopy to be 19.3 ± 2.4 nm, slightly larger than the value of 13.5 nm obtained by gradient gel electrophoresis (*6*). It is hypothesized that, during lipid binding, the apoLp-III helix bundle opens about loop regions that connect the helical segments, and helices H1, H2, and H5 become separated from helix H3 and H4 (*1*, *18*, *19*). In this "open conformation" the length of the extended protein is essentially doubled and a continuous hydrophobic surface is exposed, permitting the protein to circumscribe the periphery of the disk bilayer in a beltlike manner. Each complex, which contains five or six molecules of apoLp-III (*4*, *6*, *20*), is stabilized by interaction of the hydrophobic face of apoLp-III amphipathic helical segments with the fatty acyl chains of DMPC on the edge of the disk. A similar conformation has been proposed for lipid-bound N-terminal apoE (*14*, *21*).

The rate of *L. migratoria* apoLp-III-induced DMPC vesicle transformation into disk complexes is significantly enhanced by lowering the solution pH from 7.0 to 3.0, with the optimum pH at 3.5. The increased rate of apoLp-III-induced DMPC vesicle transformation is likely the result of pH-induced changes in apoLp-III tertiary structure, as seen for other systems (*22*). Functional and biophysical studies reveal that two pH-dependent states can be assigned, one between pH 7.2 and pH 4.0 and the other in the pH range of 4.0−3.0. At pH values between 7.2 and 4.0, although enhancement in lipid binding is seen, no changes in apoLp-III Trp fluorescence λ_{max}, aromatic CD spectral properties, or ANS fluorescence were observed. In addition, no significant changes in apoLp-III far-UV CD negative ellipticity were seen in this pH range (*6*). Taken together, these data indicate that, between pH 7.0 and pH 4.0, the secondary and tertiary structures of the apoLp-III helix bundle are largely maintained. The second phase, between pH 4.0 and pH 3.0, is characterized by important changes in apoLp-III structural properties. Fluorescence analysis revealed that, at pH 4 and lower, apoLp-III Trp residues display properties consistent with an alteration in protein tertiary structure. Furthermore, aromatic CD spectra showed that extrema at 286 and 292 nm, attributed to Trp115, collapse below pH 4.0, consistent with greater flexibility for this residue (*12*, *23*). ApoLp-III-

dependent ANS fluorescence intensity was enhanced 4-fold at pH 4 and below, indicating exposure of hydrophobic regions in the protein. Previously reported far-UV CD studies of *L. migratoria* apoLp-III as a function of pH showed that the protein resists pH-induced loss of secondary structure content over a wide range (*6*). Comparable ellipticity values were obtained at pH 7.0 and 3.2 with a maximum negative ellipticity at pH 4.5. As the solution pH is decreased below 4.0 negative ellipticity at 221 nm decreased slightly, but around pH 3 apoLp-III retains the bulk of its negative ellipticity, indicating maintenance of secondary structure content. Thus, the large red shift in Trp fluorescence λ_{max}, collapse of near-UV CD spectral extrema, and the 4-fold increase in apoLp-III-dependent ANS fluorescence intensity indicate that, between pH 4.0 and pH 3.0, significant alterations in apoLp-III tertiary structure occur. It may be considered that, at pH 3.5, the protein adopts a conformation in which its five α-helices are loosely packed, exposing hydrophobic sites. In this "loosely folded" state apoLp-III interaction with potential lipid surface binding sites is enhanced. This loosely folded protein intermediate can also be induced by destabilizing the protein with GdnHCl, resulting in increased DMPC vesicle transformation rates.

The biophysical properties of apoLp-III at pH 4.0−3.0 resemble a molten globule state, characterized by significant secondary structure but a largely disordered tertiary structure. Some features of apoLp-III show interesting similarities with pore-forming toxins of *E. coli*. The membrane binding domains of colicin A and E1 are composed of a soluble helix bundle that undergoes a large reorganization of its amphipathic α-helices upon transition to a membrane-embedded state (*24*, *25*). A pH-induced change in structure enhances binding to negatively charged phospholipid membranes (*26*) or zwitterionic phospholipid vesicles (*27*). It has been postulated that local acidic pH at the lipid interface induces a molten globule transition, enabling the protein to bind and insert into the bilayer (*27*, *28*). Binding of colicin to lipid bilayers is likely a combined effect of increased positive charge, a flexible protein conformation, and hydrophobic interactions (*9*). Similarly, low-pH-induced or GdnHCl-induced exposure of its hydrophobic interior, and/or more flexible helix packing, facilitates interaction of apoLp-III with DMPC vesicles and their transformation into disk complexes. It may be that, under pH conditions in the range of 7.0−4.0 where changes in protein structure were not detected, apoLp-III undergoes a subtle change in structure that lowers the energy barrier for interaction with lipid surfaces, as shown for channel-forming domains of colicin. Changes in the net charge of the protein that may occur within this pH range (pH 7.0−4.0) may induce subtle changes in apoLp-III structure that increase interaction with DMPC vesicles. In this pH range, studies with the unique apoLp-III from *Manduca sexta* showed hydration of Tyr and Phe residues, and this folding intermediate correlated with increased phospholipid vesicle transformation rates (*8*). Also, the ability of the N-terminal domain of human apoE3 to transform DMPC vesicles into disk complexes is pH dependent, with a strong correlation between tertiary structure alteration and increased lipid binding (*29*). The enhanced ability of *L. migratoria* apoLp-III to induce DMPC vesicle transformation at low pH is similar, in some respects, to the observation that phospholipid bilayers are more susceptible to apolipoprotein-induced transformation at their gel−liquid-crystalline phase transition temperature. In the former case, low-pH-induced alteration in protein tertiary structure organization increases its ability to interact with lipid surfaces, whereas in the latter case, temperature-induced alterations in lipid packing increase protein accessibility to the membrane surface.

ACKNOWLEDGMENT

The authors thank Robert Luty for CD analysis and Roger Bradley for electron microscopy.

REFERENCES

1. Breiter, D. R., Kanost, M. R., Benning, M. M., Wesenberg, G., Law, J. H., Wells, M. A., Rayment, I., and Holden, H. M. (1991) *Biochemistry 30*, 603−608.
2. Segrest, J. P., Garber, D. W., Brouillette, C. G., Harvey, S. C., and Anantharamaiah, G. M. (1994) *Adv. Protein Chem. 45*, 303−369.
3. Narayanaswami, V., and Ryan, R. O. (2000) *Biochim. Biophys. Acta 1483*, 15−36.
4. Wientzek, M., Kay, C. M., Oikawa, K., and Ryan, R. O. (1994) *J. Biol. Chem. 269*, 4605−4612.
5. Weers, P. M. M., Van der Horst, D. J., and Ryan, R. O. (2000) *J. Lipid Res. 41*, 416−423.
6. Weers, P. M. M., Kay, C. M., Oikawa, K., Wientzek, M., Van der Horst, D. J., and Ryan, R. O. (1994) *Biochemistry 33*, 3617−3624.
7. Raussens, V., Goormaghtigh, E., Narayanaswami, V., Ryan, R. O., and Ruysschaert J.-M. (1995) *J. Biol. Chem. 270*, 12542−12547.
8. Soulages, J. L., and Bendavid, O. J. (1998) *Biochemistry 37*, 10203−10210.
9. Zakharov, S. D., Lindeberg, M., and Cramer, W. A. (1999) *Biochemistry 38*, 11325−11332.
10. Weers, P. M. M., Wang, J., Van der Horst, D. J., Kay, C. M., Sykes, B. D., and Ryan, R. O. (1998) *Biochim. Biophys. Acta 1393*, 99−107.
11. Van der Horst, D. J. (1990) *Biochim. Biophys. Acta 1047*, 195−211.
12. Weers, P. M. M., Prenner, E. J., Kay, C. M., and Ryan, R. O. (2000) *Biochemistry 39*, 6874−6880.
13. Engelhard, M., and Evans, P. A.. (1995) *Protein Sci. 4*, 1553−1562.
14. Weisgraber, K. H. (1994) *Adv. Protein Chem. 45*, 249−302.
15. Weisgraber, K. H., Pitas, R. E., and Mahley, R. W. (1994) *Curr. Opin. Struct. Biol. 4*, 507−515.
16. Wilson, C., Wardell, M. R, Weisgraber, K. H., Mahley, R. W., and Agard, D. A. (1991) *Science 252*, 1817−1822.
17. Surewicz, W. K., Epand, R. M., Pownall, H. J., and Hui, S.-W. (1986) *J. Biol. Chem. 34*, 16191−16197.
18. Weers, P. M. M., Narayanaswami, V., Kay, C. M., and Ryan, R. O. (1999) *J. Biol. Chem. 274*, 21804−21810.
19. Narayanaswami, V., Wang, J., Kay, C. M., and Ryan, R. O. (1999) *Proc. Natl. Acad. Sci. U.S.A. 96*, 4366−4371.
20. Dettloff, M., Weers, P. M. M., Niere, M., Kay, C. M., Ryan, R. O., and Wiesner, A. (2001) *Biochemistry 40*, 3150−3157.
21. Raussens, V., Fisher, C. A., Goormaghtigh, E., Ryan, R. O., and Ruysschaert, J.-M. (1998) *J. Biol. Chem. 273*, 25825−25830.
22. Fink, A. L., Calciano, L. J., Goto, Y., Kurotsu, T., and Palleros, D. R. (1994) *Biochemistry 33*, 12504−11.
23. Strickland, E. H. (1974) *CRC Crit. Rev. Biochem. 2*, 113−175.
24. Parker, M. W., Pattus, F., Tucker, A. D., and Tsernoglou, D. (1989) *Nature 337*, 93−96.
25. Lindeberg, M., Zakharov, S. D., and Cramer, W. A. (2000) *J. Mol. Biol. 295*, 679−692.
26. Van der Goot, F. G., González-Manas, J. M., Lakey, J. H., and Pattus, F. (1991) *Nature 354*, 408−410.

27. Shin, Y.-K., Levinthal, C., Levinthal, F., and Hubbell, W. L. (1993) *Science 259*, 960−963.
28. Muga, A., González-Manas, J. M., Lakey, J. M., Pattus, F., and Surewicz, W. K. (1993) *J. Biol. Chem*. *268*, 1553−1557.
29. Weers, P. M. M., Narayanaswami, V., and Ryan, R. O. (2001) *Eur. J. Biochem.* (in press).

BI010410F